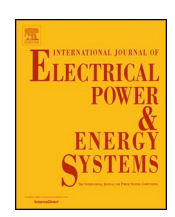
FISEVIER

Contents lists available at ScienceDirect

Electrical Power and Energy Systems

journal homepage: www.elsevier.com/locate/ijepes



A resilience assessment approach for power system from perspectives of system and component levels



Xiaonan Liu^{a,b}, Kai Hou^{a,b,*}, Hongjie Jia^{a,b}, Junbo Zhao^c, Lamine Mili^d, Yunfei Mu^{a,b}, Jusong Rim^{a,b,e}, Yunkai Lei^f

- ^a Key Laboratory of Smart Grid of Ministry of Education, Tianjin University, Tianjin, 300072, China
- ^b Tianjin Key Laboratory of Smart Energy and Information Technology, Tianjin University, Tianjin, 300072, China
- ^c The Department of Electrical and Computer Engineering, Mississippi State University, Starkville, MS 39762, USA
- ^d The Bradley Department of Electrical and Computer Engineering, Virginia Polytechnic Institute and State University, Northern Virginia Center, Falls Church, VA 22043, USA
- ^e Department of Control Science, University of Sciences, Pyongyang, DPR of Korea
- ^f State Grid Sichuan Economic Research Institute, Chengdu, Sichuan Province, 610041, China

ARTICLE INFO

Keywords: Resilience assessment System resilience indices Component resilience indices Impact-increment-based state enumeration

ABSTRACT

This paper proposes a novel resilience assessment approach for power system. Two resilience indices are developed from the perspectives of the system and individual component levels, respectively. The former one quantifies the resilience of a power system in a system-wide manner, while the latter is intended to assess the individual component through the pre-disruption and post-disruption indices. Specifically, the pre-disruption index is used to determine the weak points of the system before the occurrence of disruptions, while the post-disruption index is for designing the optimal restoration strategies. We advocate the use of impact-increment-based state enumeration method to calculate the presented indices in an efficient way without loss of accuracy. Numerical results carried out on the IEEE RTS-79 test system and the IEEE 118-bus system validate the effectiveness of the proposed approach and indices.

1. Introduction

UE to the increasing number of blackouts caused by natural disasters in the last decade, improving the resilience of power systems has become a point of focus. The low-probability-high-impact extreme disruptions may lead to the failures of multiple lines simultaneously. Therefore, the traditional scenario-based reliability analysis that is hinged on the expected energy-not-served and the N-1 criterion does not assess the resilience of the system to low probability but high impact extreme events [1,2]. The latter may result in cascading failures leading to large-scale outages and the destruction of part of the power infrastructure. A literature review on risk assessment of cascading failures leading to blackouts is provided in a recent IEEE Task Force paper [3].

The concept of resilience was first introduced for ecological systems by Holling [4]. Specifically, he defines resilience of an ecological system as its ability to move far away from equilibria due to disturbances without changing its structure. This work has triggered a

growing research activity on resilience in social [5], and engineering systems [6], among others. Following Mili et al. [7], we define the resilience as the ability of a system subjected to a class of unexpected extreme disturbances to degrade gracefully, and to recover its function through emergency or restorative actions once the disturbances have ceased. This definition of resilience is contrasted with the concept of robustness to a given class of disturbances, which is defined as the ability of a system to maintain its functionality when it is subjected to a disturbance of that class. A measure of robustness is the reliability of a system, defined as the probability that a system is able to retain, over a long time period, its intended function under given conditions when it is subjected to internal or external failures.

With the ever-increasing focus on enhancing the resilience of a power system to extreme events, there is a critical need to develop the related quantitative approaches and indices. Several resilience metrics for infrastructures have been proposed in [8–21]. The so-called "resilience triangle", was first introduced by Bruneau [8] to assess seismic resilience of community system. With this "triangle", resilience can be

E-mail addresses: xiaonanliu@tju.edu.cn (X. Liu), hdbhyj@tju.edu.cn (K. Hou), hjjia@tju.edu.cn (H. Jia), junbo@ece.msstate.edu (J. Zhao), lmili@vt.edu (L. Mili), yunfeimu@tju.edu.cn (Y. Mu), jsrim@tju.edu.cn (J. Rim), yklei@tju.edu.cn (Y. Lei).

^{*} Corresponding author. Tel.: +8615822945162.

Nome	enclature	$Q_1(t)$ declined load s	supply after disruptions
		v_m design wind sp	peed of the <i>m</i> th line
Indice	s and sets	$\lambda_m(t)$ failure rate of	the <i>m</i> th line at time <i>t</i>
		a_m , b_m model parame	ters
i, m	index of the lines	l_m length of the n	nth line
t	index of time periods	I_s impact of the f	failure scenario s
\boldsymbol{A}	set of all lines	T_s duration of the	e failure scenario s
s_m	set of failed lines, including the mth line	f_s frequency of the frequency of the frequency of the frequency f_s	he failure scenario s
s_0	set of failed lines without the mth line	P_s probability of	the failure scenario s
Ω_s	set of possible failure scenarios	$R_{\rm sys} u_{m=0}$ system resilien	nce index under $u_m = 0$
		$R_{m,pre}$ pre-disruption	component resilience index of the <i>m</i> th line
Variab	oles and parameters		n component resilience index of the <i>m</i> th line
		u_m failure probab	ility of the <i>m</i> th line
$r_1, r_2,$	R_{sys} indices of system resilience	Ω_A^k kth order subs	et of A
$v_m(t)$	wind speed of the <i>m</i> th line at time <i>t</i>	ΔI_s impact-increm	ent of failure scenario s
$Q_0(t)$	load supply under normal state	•	

quantified as the integral of the system performance degradation with time after disruptions [9,10]. However, it cannot be used to measure the duration of the performance degradation before the recovery. To address that, Panteli [11] proposed a multi-phase "resilience trapezoid", which extends the "resilience triangle" to consider the different phases that a power system may experience during the disruption. It is worth noting that the aforementioned approaches and indices are intended for a specific failure scenario after disruptions. In view of the unpredicted failure scenarios before disruptions, Panteli [12-15] assessed the resilience by quantifying the frequency, duration and number of customer disconnections before the system suffering disruptions. Those indices were then used to evaluate the effectiveness of different resilience-enhancement methods. Since disruptions may occur more than once in a long period [16-18], Ouyang introduced a timedependent expected annual resilience indices based on the trapezoid. Amirioun [19–22] quantified the system resilience from the perspective of supplied load degradation against weather-oriented events. However, the duration and impact of failure states for multiple transmission line outages are not investigated [23].

A power system may suffer from various types of disruptions, such as natural disasters and terrorist attacks [24]. As a result, the frequencies, durations, and impacts of different disruptions should be taken into account simultaneously when assessing the entire system resilience, yielding heavy computational burden. Note that the direct impacts of those disruptions on power system are the failures of important components, which further result in overloads, voltage violations, and load shedding, among others. The traditional power system reliability assessment aims at measuring the capacity of the system to meet the load demands over a long period of time. Generally, the failure probabilities of components are treated as constants, which can be obtained from historical data. Conversely, resilience of a power system focuses on its capacity to maintain its performance in a short period of time under extreme disruptions. Due to the abrupt change of external environment, the failure probabilities of components will increase dramatically when disruptions occur. This paper develops an effective quantitative resilience assessment approach and indices with the consideration of various failure scenarios caused by extreme disruptions. Compared with reliability assessment, the failure probability of transmission lines in resilience assessment is much higher. Thus, there are more high-order failure scenarios and to deal with that, an impact-increment-based state enumeration (IISE) method developed in our previous work [25-28] is extended to calculate the proposed indices in an efficient manner without loss of accuracy. Furthermore, two resilience indices are developed from the perspectives of the system and individual component levels, respectively. The former one quantifies the resilience of a power system in a system-wide manner, while the latter is intended to assess the individual component through the predisruption and post-disruption indices. They allow us to evaluate the contribution of each component to the resilience of the system from the perspectives of prevention and restoration. Finally, comparative results with other alternatives show that the proposed approach yields more accurate results while maintaining higher computational efficiency.

The rest of the paper is organized as follows. Section 2 introduces the proposed system resilience assessment approach and indices. Then, the proposed pre-disruption and post-disruption component resilience indices are developed in Section 3. Numerical results are presented and analyzed in Section 4, and conclusions are drawn in Section 5.

2. System resilience assessment indices

In power systems, load shedding has been widely recognized as the disturbance that directly impacts the effectiveness of the recovery process [29]. From the perspective of the system resilience index proposed by Bruneau [8], the system performance can be defined as the load supply at any time t, as depicted in Fig. 1. Then, the system resilience can be quantified as

$$r_1 = \int_{t_0}^{t_1} \left[Q_0(t) - Q_1(t) \right] dt \tag{1}$$

$$r_2 = \int_{t_0}^{t_1} Q_1(t)dt / \int_{t_0}^{t_1} Q_0(t)dt$$
 (2)

where r_1 and r_2 can both denote the system resilience index under a specific disruption; $Q_0(t)$ denotes the load supply under normal state. After the disruption occurs, the load supply $Q_1(t)$ may decline and then return to the normal level after a period of time $t=t_1$ - t_0 . The index r_1 represents the performance degradation during the disruption, while the index r_2 shows the ratio of the maintained performance to the degraded performance. Although the two indices are in different forms, their essence is similar. They can be used to assess the overall system resilience under a specific disruption. Note that the more resilient the system is, the smaller the shadow area will be.

The above indices can be applied to assess the system resilience of an identified failure scenario after a particular disruption. However, the failure scenario cannot be accurately predicted before disruptions. A feasible solution is to take into account all possible failure scenarios

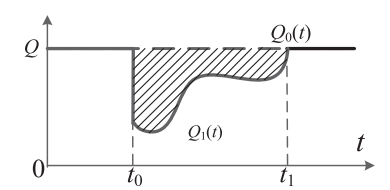


Fig. 1. The resilience triangle.

that may result from the extreme disruptions. Hence, the system resilience indices can be expressed as the multiplication of the probabilities and performance degradations of all possible failure scenarios under extreme disruptions. Our previously developed IISE method is introduced to improve the accuracy and efficiency of resilience assessment.

The resilience assessment approach and indices should be applicable to any types of natural disasters, as long as the corresponding relationship between component failure probability and weather intensity is obtained. Without loss of generality, this paper takes typhoon as an example to assess the resilience of power system. It should be noted that the cables are buried underground and transformers usually have high structural reliability against typhoon. Therefore, it is assumed that only the failure rates of overhead transmission lines will be affected by typhoon. For instance, the typhoon DAMREY hit Hainan Province of China in 2005, and damaged 336.8 km of overhead transmission lines while no cable or transformer outage happened. In the presence of typhoon, the modified failure probability $u_m(t)$ of mth transmission line under different wind speed can be expressed as follows [30]:

$$\lambda_m(t) = e^{\left(a_m \frac{v_m(t)}{v_m} + b_m\right) l_m} \tag{3}$$

$$u_m(t) = 1 - \exp\left(-\int_0^t \lambda_m(\mu)d\mu\right) \tag{4}$$

where $v_m(t)$ represents the wind speed at time t, v_m represents the design wind speed of the mth line, $\lambda_m(t)$ represents the failure rate of the mth line at time t, a_m and b_m are the model parameters, which can be obtained by statistical analysis of historical data, l_m represents the length of the mth line. It is noted that the duration of the dynamic process is much shorter than the repair/restoration process. Thus it is assumed that the performance function degrades immediately when transmission lines fail, and recovers immediately when the failed lines are repaired. If information on the restoration is available, then more accurate restoration process can be built. In order to further simplify the computation process, the portion of degraded performance function is approximated as a rectangle, as shown in Fig. 2.

The system resilience index can be expressed as the expected impact of potential failure scenarios that may occur under a particular extreme disruptions. Formally, we have the system resilience index as follows. Based on the frequency and duration (FD) method, the relationship of the failure probability P_s , the failure frequency f_s and the failure duration time T can be obtained via [31].

$$R_{sys} = E\left(\int_{t_0}^{t_1} [Q_0(t) - Q_1(t)]dt\right) \approx \sum_{s \in \Omega_s} f_s I_s T_s = \sum_{s \in \Omega_s} P_s I_s$$
 (5)

where Ω_s represents the set of possible failure scenarios caused by the extreme disruptions, I_s represents the initial performance degradation due to failure scenario s, T_s represents the duration of the degrade state due to the failure scenario s, f_s represents the frequency of failure scenario s, $I_s I_s$ shows the approximate impact area, P_s represents the probability of the failure scenario s, which can be further expressed as

$$P_{s} = \prod_{m \in s} u_{m} \prod_{n \notin s} (1 - u_{n})$$

$$\tag{6}$$

where $m \in s$ indicates that component m fails in scenario s, u_m and u_n can be obtained by (4).

It can be seen from (5) that the resilience assesses system response to extreme disruptions, while the reliability focuses on normal disturbances. Therefore, the resilience assessment has to deal with higher-order failure scenarios. However, the workload of the state enumeration (SE) method is tremendous for the resilience assessment because of the vast number of high-order failure scenarios. Note that if all failure scenarios are enumerated, SE would obtain the most accurate results.

However, as the number of system components increases, the number of system states grows exponentially. This will make it impossible for the SE method to enumerate all failure scenarios. In order to alleviate the computational burden, the higher order failure scenarios have been ignored by the SE method, yielding decreased accuracy. By contrast, in the IISE method, the impacts of higher-order failure scenarios have been strategically transferred into the corresponding lower order ones. As a result, IISE obtains better results than the SE method while keeping similar computational efficiency. The schematic diagram of the IISE method is shown in Fig. 3. More details of the IISE method can be found in [25].

In this paper, the IISE method is extended to calculate the component resilience indices efficiently, which will be explained later. Formally, the power system resilience indices with M lines is obtained via

$$R_{\text{sys}} = \sum_{k=0}^{M} \sum_{s \in \Omega_A^k} (P_s I_s) = \sum_{k=0}^{M} \sum_{s \in \Omega_A^k} (\prod_{i \in s} u_i \prod_{i \notin s} (1 - u_i)) I_s$$

$$= \sum_{k=0}^{M} \sum_{s \in \Omega_A^k} (\prod_{i \in s} u_i) \Delta I_s$$
(7)

where u_i represents the failure probability of ith line that is related to the failure scenario s, A is the set of all M lines and Ω_A^k represents the k order subset of A, and ΔI_s is the impact-increment of load shedding of failure scenario s.

3. Component resilience assessment indices

In additional to the indices of the entire system, resilience assessment should also be conducted on component level so as to locate the most influential lines. To this end, two indices, namely the pre-disruption and the post-disruption component resilience indices, are proposed from the perspective of individual lines. Those indices can be used to assess the potential damage of a particular line failure on the overall resilience of the system, and help planners and operators seek for resilience enhancement strategies.

3.1. Pre-disruption component resilience indices

Before an extreme disruption occurs, operators are expected to use some indices to find out the weak points of the system. To tackle this issue, pre-disruption component resilience indices are defined as the contribution of a particular line failure on the overall system resilience. For a system with M lines, the pre-disruption component resilience index $R_{m,pre}$ with respect to the line m can be obtained as

$$R_{m,pre} = R_{sys} - R_{sys}|_{u_m=0}$$
(8)

where $R_{\rm sys}$ represents the system resilience index; u_m is the failure probability of the mth line; $R_{\rm sys}|u_{m=0}$ is the system resilience index under the condition, i.e., $u_m=0$.

It is worth noting that $R_{\rm sys}|u_{m=0}$ can be directly obtained after the system resilience indices $R_{\rm sys}$ is calculated, because the failure probability of each transmission line and the impact-increment of each

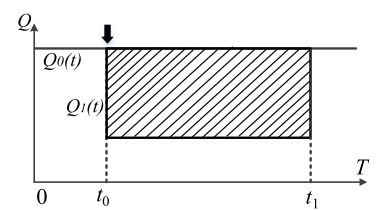


Fig. 2. The resilience rectangle.

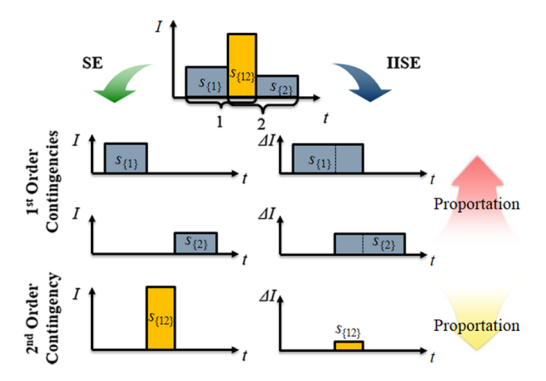


Fig. 3. The schematic diagram of the IISE method.

failure scenario have been obtained during the calculation process of system resilience index. For a system with M transmission lines, R_{sys} can be divided into the following two parts:

$$R_{sys} = \sum_{k=0}^{M} \sum_{s \in \Omega_{A}^{k}} (\prod_{i \in s} u_{i}) \Delta I_{s}$$

$$= u_{m} \sum_{k=0}^{M} \left[\sum_{\substack{s_{m} \in \Omega_{A}^{k} \\ m \in s_{m}}} (\prod_{i \in s} u_{i}) \Delta I_{s_{m}} \right] + \sum_{k=0}^{M} \left[\sum_{\substack{s_{0} \in \Omega_{A}^{k} \\ m \notin s_{0}}} (\prod_{i \in s_{0}} u_{i}) \Delta I_{s_{0}} \right]$$

$$(9)$$

where s_m represents the failure scenario denoted by a set of corresponding failed lines, including the mth line while s_0 represents a failure scenario that excludes the mth line. Then $R_{sys}|u_{m=0}$ can be calculated via

$$R_{\text{sys}}|_{u_{m}=0} = \sum_{k=0}^{M} \sum_{s \in \Omega_{A}^{k}} (\prod_{i \in s} u_{i}) \Delta I_{s}|_{u_{m}=0} = \sum_{k=0}^{M} \left[\sum_{\substack{s_{0} \in \Omega_{A}^{k} \\ m \notin s_{0}}} (\prod_{i \in s_{0}} u_{i}) \Delta I_{s_{0}} \right]$$
(10)

By subtracting (9) from (10), all the impact-increments that are not related to the mth line are eliminated. Therefore, $R_{m,pre}$ can be obtained through

$$\begin{split} R_{m,pre} &= R_{sys} - R_{sys}|_{u_m = 0} = \sum_{k=0}^{M} \sum_{s \in \Omega_A^k} (\prod_{i \in s} u_i) \Delta I_s - \sum_{k=0}^{M} \sum_{s \in \Omega_A^k} (\prod_{i \in s} u_i) \Delta I_s|_{u_m = 0} \\ &= u_m \sum_{k=0}^{M} \left[\sum_{\substack{sm \in \Omega_A^k \\ m \in s_m}} (\prod_{i \in s} u_i) \Delta I_{s_m} \right] \end{split}$$

where ΔIs_m can be found in (9) while $R_{m,pre}$ can be directly obtained from (11) without additional OPF calculations. In the Appendix, the 3-bus system is used to elaborate the IISE based calculation process of the pre-disruption component resilience indices.

After identifying the weak points of the system, planners and operators can determine the enhancement strategies accordingly to improve the system resilience. The enhancement measures include but are not limited to building redundant lines, upgrading the materials of the transmission lines, re-routing transmission lines to areas that are less affected by natural disasters [32,33]. Further research will be conducted in the future.

3.2. Post-disruption component resilience indices

Obviously, it is difficult to make a power system resilient to all potential extreme disruptions. However, resilience assessment and management for a faster recovery can be executed before a disaster strikes. They allow corrective, emergency, and restorative actions to be taken in a timely manner from performance degradation viewpoint, given the resources that have been deployed on the system. Note that corrective actions are typically control actions executed to bring back the system to equilibrium while the system is maintaining its integrity; emergency actions include islanding as well as load and generation shedding to avoid a large-scale blackout; and restorative actions are those taken to fix damaged equipment and to restore the functionality of the system. Therefore, in addition to the resistance capability before disruptions, system corrective and recovery capability during and after the disruptions should also be evaluated. Regarding the restorative actions executed after extreme disruptions, they include the restoration of the failed lines, transformers, and any damaged equipment in the substations. This should be carried out as quickly as possible so that the economic losses endured by the society are minimized. However, due to the limitation of available maintenance crews and resources, it is unlikely that all the damaged equipment can be repaired at the same time. Therefore, the resilience of various restorative strategies are not the same. In fact, it is a matter of concern for the operators to determine the repair priority of the failed components in different failure scenarios. Note that the pre-disruption component resilience indices are calculated before the disruptions have occurred by considering the worstcase scenario.

In this paper, we develop post-disruption component resilience indices for system restoration. Similarly, the IISE method can be used to quickly calculate the post-disruption component resilience indices. For a system with M lines, the post-disruption component resilience index of the mth line under a certain failure scenario s can be obtained by

$$R_{m,post} = R_{sys}|_{\substack{u_i = 1, i \in \Omega_s: \\ u_j = 0, j \notin \Omega_s}} - R_{sys}|_{\substack{u_m = 0; \\ u_i = 1, i \neq m | i \in \Omega_s: \\ u_j = 0, j \notin \Omega_s}} = \sum_{s_m \in \Omega_m \in s} \Delta I_{s_m}$$
(12)

where Ω_s is denoted by a set of failed lines under failure scenario s, Ω_{mes} is the subset of Ω_s that contains mth line. Similar to the pre-disruption indices, ΔIs_m and $R_{m,post}$ can be obtained accordingly.

For a given failure scenario, the failed line with the highest postdisruption component resilience index has the highest priority to be repaired. However, after it is repaired, the post-disruption component resilience indices of all unrepaired lines will change and have to be recalculated. Thus, the post-disruption component resilience indices need to be updated repeatedly to determine the optimal recovery strategy. In each loop, the line with the highest post-disruption component resilience index is prioritized for repair.

The repair priority of failed lines under a specific failure scenario can be obtained by executing the following steps:

Step 1: Identify the failed lines and record the initial failure scenario *s*. Initialize maintenance counter k = 1.

Step 2: Compute the post-disruption component resilience indices of all failed lines given by (12).

Step 3: Search the maximum index and record its line number i. The ith line is repaired at the kth rank.

Step 4: Exclude the *i*th line from Ω_s .

Step 5: If $card(\Omega_s) > 1$, where $card(\Omega_s)$ represents the cardinality of Ω_s , set k = k + 1 and go back to Step 2; Otherwise, go to Step 6.

Step 6: Output rank *k* and its corresponding line number *i*.

To demonstrate the above procedures, we take the 3-bus system as an example by assuming that it suffers from an extreme disruption that leads to the failures of all three lines. In the case of limited maintenance resources, only one line can be repaired at a time. Because different repair sequences correspond to different degree of system recovery, it is necessary to determine the optimal recovery strategy by using the

(11)

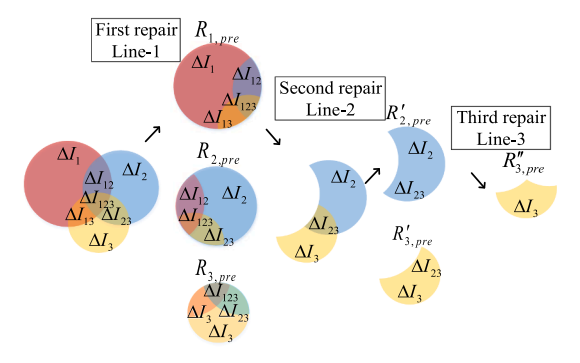


Fig. 4. Computation process of the post-disruption resilience indices.

proposed post-disruption component resilience indices. As shown in Fig. 4, the red, blue and yellow circles respectively represent the contribution of Line-1, Line-2 and Line-3 to the total system impact, and the overlaps represent the increment-impact of multiple failures. All lines can be ranked in accordance with the results of the post-disruption component resilience indices. It can be seen that Line-1 has the largest value of the index; so it should be repaired with the highest priority. The optimal recovery strategy can be determined by repeating ranking process. The detailed computation process is shown in the Appendix.

3.3. Resilience assessment framework for system restoration

The overall resilience assessment framework is shown in Fig. 5. The proposed framework assesses the system resilience at both the system and component levels. The latter consists of pre-disruption and postdisruption component resilience indices. Before the occurrence of extreme disruptions, the system resilience indices can be used to quantify and assess the resilience of the entire system. It should be noted that the failure probability of each line will dramatically increase under extreme weather scenario. As a result, it is necessary to correct the failure probability according to the weather intensity. For a system that is not resilient, the weak points can be then identified by the pre-disruption component resilience indices, and the corresponding enhancement measures can be carried out in the face of upcoming or future extreme disruptions. After the extreme disruptions occur, a large number of lines may fail. With the post-disruption component resilience indices, the effective recovery strategies can be initiated to prioritize the repair of damaged components.

4. Numerical results

4.1. Case I: IEEE RTS-79 system

The proposed approach and indices are first tested in the IEEE RTS-79 system. Details of this system can be found in [34]. Monte Carlo simulations (MCS) [35] are used as a benchmark, and the traditional SE method is implemented for comparison. For MCS, the failure probability of each transmission line is assumed. The failure probability under each failure scenario is generated from the state sampling of each line. The state of each line can be determined by sampling the failure probability distribution of the line. It is assumed that each line has both failure and normal operation states, and the failure of each line is independent of each other. As a typical type of extreme disruption, typhoon is utilized to test the performance of the above methods. Based on the reference [30], the modified failure probability can be obtained according to the wind profile. To be more specific, the wind speed is set to 40 m/s in this paper based on the definition of a typhoon given by the World Meteorological Organization. It is notable that cables and transformers usually have high structural reliability against typhoon, so

we only consider the failure of transmission lines in the studies. All simulations are executed by MATLAB on a PC with Intel Core i5 CPU @ $3.20~\mathrm{GHz}$ and $8~\mathrm{GB}$ RAM.

4.2. Accuracy and efficiency of the proposed approach

The performances of the SE and IISE methods are tested in this section under normal condition and extreme disruption, respectively. The MCS case with 10⁶ sampled failure scenarios is regarded as the benchmark. The results of system resilience indices and their relative errors are listed in Table 1, where SE; and IISE; represent the result obtained by the SE method and IISE method considering the 1st to i^{th} order failure scenarios, respectively. The enumerated order of the SE method and the IISE method are extend to 6th order. It can be seen that the calculation times of the two methods are similar, but the IISE method is more accurate than the SE method, especially in the extreme situation. This is because the failure probabilities of transmission lines increases dramatically when the typhoon has arrived, so the probabilities of high-order failure scenarios are enhanced accordingly. However, those high-order ones cannot be enumerated by the SE method, which results in large errors. The IISE method, by contrast, strategically transfers the impacts of high-order failure scenarios into the corresponding lower-order ones. In other words, the impacts of high-order failure scenarios are well considered even though they are not enumerated, yielding more accurate results. As discussed in Section II, the higher order failure scenarios have been ignored by the SE method, yielding decreased accuracy. When the number of damaged lines increases, the accounted number of failure scenarios increases, i.e., more scenarios are enumerated. That is why the error is decreased. By contrast, in the IISE method, the impacts of higher-order failure scenarios have been strategically transferred into the corresponding lower order ones. As a result, IISE obtains better results than the SE method. In addition, it can also be found that the time consumption of the IISE method is far less than that of the MCS method. Thus, the accuracy and efficiency of the proposed approach and indices are verified.

4.3. Pre-disruption analysis

Before the occurrence of an extreme disruption, the values of the pre-disruption resilience indices can be calculated to locate the weak points of the system. The pre-disruption resilience indices induced by different weather intensities are calculated, as shown in Table 2. It can be seen that when the extreme disruptions occur, the indices increase significantly. This is because transmission lines are more likely to fail in extreme situations. It can also be found that the indices of some certain

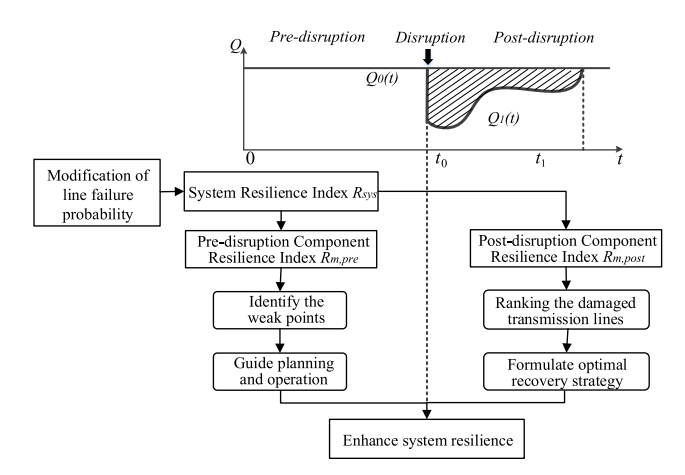


Fig. 5. The proposed resilience assessment framework.

Table 1
The Proposed System Resilience Indices of the RTS-79 Test System.

Methods	Normal	Normal			Extreme		
	R _{sys} (MWh)	Error (%)	Time (s)	R_{sys} (MWh)	Error (%)	Time (s)	
Benchmark	0.0263	_	1.77e4	0.7375	-	1.71e4	
SE1	0.0256	2.6616	1.27e0	0.4761	35.4441	1.00e0	
SE2	0.0261	0.7605	1.11e1	0.6822	7.4983	1.09e1	
SE3	0.0261	0.7605	1.06e2	0.7245	1.7627	1.02e2	
SE4	0.0261	0.7605	9.24e2	0.7299	1.0305	8.64e2	
SE5	0.0261	0.7605	3.41e3	0.7304	0.9627	3.38e3	
SE6	0.0261	0.7605	2.29e4	0.7304	0.9627	2.27e4	
IISE1	0.0260	1.1407	1.54e0	0.6697	9.1932	1.50e0	
IISE2	0.0261	0.7605	1.18e1	0.7327	0.6508	1.15e1	
IISE3	0.0261	0.7605	1.08e2	0.7351	0.3254	1.05e2	
IISE4	0.0261	0.7605	1.52e3	0.7352	0.3119	1.49e2	
IISE5	0.0261	0.7605	3.67e3	0.7352	0.3119	3.63e3	
IISE6	0.0261	0.7605	2.44e4	0.7352	0.3119	2.43e4	

 Table 2

 The Pre-disruption Component Resilience Indices.

Normal		Extreme		
Line	$R_{m,pre}(MWh)$	Line	$R_{m,pre}(MWh)$	
27 (bus 15 to 24)	0.0228	27 (bus 15 to 24)	0.5958	
5 (bus 2 to 6)	0.0032	5 (bus 2 to 6)	0.1082	
23 (bus 14 to 16)	4.53e-5	23 (bus 14 to 16)	0.0205	
19 (bus 11 to 14)	4.52e-5	19 (bus 11 to 14)	0.0192	

lines are remarkably larger than others, indicating that the failures of those lines may results in more severe consequences. Therefore, operators should pay more attention to the lines with high indices so as to enhance the system resilience against extreme disruptions. It is also worth noting that after $R_{\rm sys}$ is obtained, the pre-disruption component resilience indices can be directly calculated by (11). Therefore, the pre-disruption analysis will bring no more computation burden, which is another advantage of the proposed approach. According to the results, the pre-disruption component resilience indices of Line-27 and Line-5 are much larger than others, that is, the failure of Line-27 or Line-5 will cause relatively large load shedding. The operators should pay more attention on those lines before the extreme disruptions occur.

4.4. Post-disruption analysis

The post-disruption component resilience indices can be used to optimize recovery strategies after the occurrence of an extreme disruption. In order to illustrate the benefits of the proposed post-disruption component resilience indices, we assume that Line-5, Line-27, Line-19 and Line-23 fail after the typhoon has arrived, and the post-disruption indices of this failure scenario are calculated. As shown in Tables 3 and 4, a higher post-disruption index implies a higher repair priority, which means that repairing the line with higher index results in more load recovery. When the post-disruption indices of some lines are identical, whichever line for repair/restoration first is feasible. It should be noted that once the first candidate line for repair is selected, the followed recovery strategy is not in accordance with the indices ranking computed under the initial failure scenario. In other words, the post-disruption component resilience indices of the remaining failed lines should be repeatedly computed in each step. In addition, if the post-disruption component resilience indices of two lines are equivalent, their repair priority may affect the subsequent repair sequences. Since $R_{19,post}$ has the same value as $R_{23,post}$, different recovery strategies

under this scenario are studied. As shown in Tables 3 and 4, the post disruption indices of Line-19 and Line-23 are equivalent, but their subsequent repair sequences are different. The post-disruption component resilience indices of each lines in each recursive step are computed when Line-19 and Line-23 are first repaired, respectively. From the results, we observe that the optimal recovery strategies are 19-27-5-23 or 23-27-5-19; see the last line of Tables 3 and 4 for more details.

To verify the necessity of the post-disruption resilience indices and their usage for the optimal recovery strategy, the following two cases are studied:

- (a) Case 1: Only one group of maintenance crew is available while the mean repair duration of each transmission line is set to 10 h [11]. Note that the determination of an accurate value for the transmission line repair needs to consider various factors. For example, the difficulty of the repair crews to access the area of the damaged line will extend the restoration time. Since there does not exist a suitable probability model to obtain the restoration time, the mean repair time to assess the post-disruption resilience is adopted. All twenty four recovery strategies are compared under this scenario.
- (b) Case 2: Two group of maintenance crews are available while the mean repair duration of each transmission line is set to 10 h. All six recovery strategies are compared under this scenario.

Furthermore, it is assumed that: (1) the crew is dispatched with no delay as soon as the failures occur; (2) the network becomes fully functional as long as the failed transmission lines are repaired; (3) the duration of failure transient can be neglected with respect to the time of repair.

All possible recovery strategies and their corresponding system resilience indices r_2 are calculated and shown in Tables 5 and 6 in a descending order. It is observed from Table 5 that the optimal recovery strategies are 19-27-5-23 and 23-27-5-19 in Case 1 as they achieve the best system resiliences. Note that they are formulated according to the

Table 3
The Post-disruptions Component Resilience Indices , in Each Recursive Step When Line 19 is Selected for First Repair.

First	Second	Third	Fourth
19.18 MW	18.64 MW	5.89 MW	_
195 MW	_	-	-
195 MW	0.01 MW	0 MW	-
57.41 MW	56.87 MW	_	0 MW
Line 19	Line 27	Line 5	Line 23
	19.18 MW 195 MW 195 MW 57.41 MW	19.18 MW 18.64 MW 195 MW – 195 MW 0.01 MW 57.41 MW 56.87 MW	19.18 MW 18.64 MW 5.89 MW 195 MW 195 MW 0.01 MW 0 MW 57.41 MW 56.87 MW -

Table 4The Post-disruptions Component Resilience Indices , in Each Recursive Step When Line 23 is Selected for First Repair.

Indices	First	Second	Third	Fourth
$R_{5,post}$	19.18 MW	18.65 MW	5.89 MW	-
$R_{19,post}$	195 MW	0.02 MW	0 MW	-
$R_{23,post}$	195 MW	-	-	-
$R_{27,post}$	57.41 MW	56.88 MW	-	0 MW
Repair Priority	Line 23	Line 27	Line 5	Line 19

Table 5System Resilience of Each Recovery Strategy with One Crew.

Strategy	r ₂ (%)	Strategy	r ₂ (%)	Strategy	r ₂ (%)
19-27-5-23	96.19	19-5-23-27	95.22	5-19-27-23	93.69
23-27-5-19	96.19	23-5-19-27	95.22	5-23-27-19	93.69
19-27-23-5	96.12	19-23-5-27	95.01	5-19-23-27	93.17
23-27-19-5	96.12	23-19-5-27	95.01	5-23-19-27	93.17
19-5-27-23	95.74	27-23-5-19	94.58	27-5-19-23	92.38
23-5-27-19	95.74	27-19-5-23	94.58	27-5-23-19	92.38
19-23-27-5	95.45	27-23-19-5	94.51	5-27-19-23	91.94
23-19-27-5	95.45	27-19-23-5	94.51	5-27-23-19	91.94

Table 6System Resilience of Each Recovery Strategy with Two Crews.

Strategy	r_2 (%)	Strategy	r_2 (%)	Strategy	r ₂ (%)
19&27-5&23	97.69	5&19-23&27	97.36	19&23–5&27	97.19
23&27-5&19	97.69	5&23-19&27	97.36	5&27–19&23	96.04

post-disruption component resilience indices. By comparison, the recovery strategy 27-5-23-9, which is formulated according to the predisruption component resilience indices under different wind speeds, is not the optimal one. The same conclusion can be drawn for the Case 2. As shown in Table 6, the optimal recovery strategies 19&25-5&23 and 23&27-5&19 make the system more resilient than other strategies, such as 5&27-9&23. From Tables 5 and 6, we can achieve a best system resilience if the repair sequence is formulated according to the ranking results of prost-disruption component resilience indices. Furthermore, accelerateing the repair speed will lead to much better system resilience.

As a result, it is clear that the proposed post-disruption component resilience indices are able to provide useful information for making recovery strategies and enhancing the system resilience. It is important to note that although the equivalent post-disruption component resilience indices may affect the repair sequence, they have almost no effect on the overall system resilience. In Case 1, the system resiliences of recovery strategies 19-27-5-23 and 23-27-5-19 are 96.19%. These values are 97.69% for the recovery strategies 19&25-5&23 and 23&27-5&19 in case 2.

Table 7The Proposed System Resilience Indices of the IEEE-118 System.

Methods	Normal	Normal			Extreme		
	R _{sys} (MWh)	Error (%)	Time (s)	R_{sys} (MWh)	Error (%)	Time (s)	
Benchmark	0.0456	-	7.75e4	0.3868	_	7.06e4	
SE1	0.0424	7.01754	15.1794	0.0744	80.7654	15.1380	
SE2	0.0454	0.43860	1.26e3	0.1985	48.6815	1.17e3	
SE3	0.0455	0.21930	5.95e4	0.2998	22.4922	5.85e4	
IISE1	0.0454	0.43860	20.9470	0.3241	16.2099	19.4280	
IISE2	0.0456	0.06871	1.27e3	0.3878	0.2585	1.21e3	
IISE3	0.0456	0.06868	5.96e4	0.3880	0.3102	5.87e4	

Table 8The Results of Resilience Indices of IEEE-118 Test System.

Normal		Extreme		
Line	$R_{m,pre}(MWh)$	Line	$R_{m,pre}(MWh)$	
183 (bus 68 to 116) 184 (bus 12 to 117) 125 (bus 79 to 80) 121 (bus 77 to 78)	0.0281 0.0085 0.0045 0.0043	184 (bus 12 to 117) 125 (bus 79 to 80) 183 (bus 68 to 116) 121 (bus 77 to 78)	0.2049 0.0711 0.0299 0.0174	

Table 9The Post-disruptions Component Resilience Indices in Each Recursive Step When Line 121 is Selected for First Repair.

Indices	First	Second	Third	Fourth
R _{121,post} R _{125,post} R _{183,post} R _{184,post} Repair Priority	110 MW	-	-	-
	110 MW	0 MW	0 MW	13.35 MW
	84 MW	84 MW	-	-
	20 MW	20 MW	6.65 MW	-
	Line 121	Line 183	Line 184	Line 125

4.5. Case II: IEEE 118-Bus system

Case studies are also conducted on the IEEE 118-bus test system to further validate the performance of the proposed approach. Detailed information of this system can be found in [36]. Lengths of all transmission lines are assumed to be proportional to their impedances. Likewise, the transformers have high structural reliability against typhoon and only the damage of transmission lines are considered.

4.5.1. Accuracy and efficiency of the proposed approach

In a similar way to the previous case, the system resilience indices of various methods in the presence of normal condition and extreme disruptions are tested, and the results are shown in Table 7. It can be found that the IISE method can still maintain its accuracy subject to different weather intensity and different failure scenarios. Meanwhile, the computing times of IISE method are far less than MCS method. Thus, the accuracy and efficiency of the proposed approach and indices are also verified in a larger-scale system.

4.5.2. Pre-disruption analysis

Similar to the 79 bus system case, the pre-disruption resilience indices under normal condition and extreme disruption are calculated and they are shown in Table 8. It can be seen that the indices have remarkably increased with the weather intensity. In particular, the pre-disruption index of Line-184 under extreme disruption is increased the most as compared to that under normal condition. This is because the length of Line-184 is longer than the other three lines and its failure probability surges under extreme disruption according to (4). Moreover, it can be found that the rank of the pre-disruption resilience

Table 10
The Post-disruptions Component Resilience Indices in Each Recursive Step When Line 125 is Selected for First Repair.

Indices	First	Second	Third	Fourth
$R_{121,post}$	110 MW	0 MW	0 MW	15.92 MW
$R_{125,post}$	110 MW	-	-	-
R _{183,post}	84 MW	84 MW	-	-
$R_{184,post}$	20 MW	20 MW	4.08 MW	-
Repair Priority	Line 125	Line 183	Line 184	Line 121

Table 11
System Resilience of Each Recovery Strategy with One Crew.

Strategy	r ₂ (%)	Strategy	r ₂ (%)	Strategy	r ₂ (%)
121-183-184–125	97.24	121-184-183-125	96.74	184-121-183-125	96.03
125-183-184-121	97.24	125-184-183-121	96.72	125-121-184-183	96.02
125-183-121-184	97.19	125-121-183-184	96.53	121-125-184-183	96.02
121-183-125-184	97.19	121-125-183-184	96.53	184-125-183-121	96.01
183-121-184-125	97.03	183-184-121-125	96.33	184-183-121-125	95.82
183-125-184-121	97.01	183-184-125-121	96.31	184-183-125-121	95.80
183-125-121-184	96.98	125-184-121-183	96.18	184-125-121-183	95.47
183-121-125-184	96.98	121-184-125-183	96.18	184-121-125-183	95.47

Table 12System Resilience of Each Recovery Strategy with Two Crews.

Strategy	r_2 (%)	Strategy	r_2 (%)	Strategy	r ₂ (%)
121&183-125& 184	98.62	121&184-125& 183	98.24	121&125-183& 184	98.12
125&183-121& 184	98.62	125&184-121& 183	98.24	183&184-121& 125	98.09

indices are different under different weather intensities. Therefore, the operators should recalculate the pre-disruption indices when the weather intensity changes, and pay more attention to the lines with the largest indices. The recalculation can be efficiently conducted using the IISE method because the pre-disruption indices are directly obtained by (11).

4.5.3. Post-disruption analysis

In order to demonstrate the benefits of the post-disruption component resilience indices in the application of a larger-scale systems, we assume that Line-121, Line-125, Line-183 and Line-184 fail after the typhoon. Since $R_{121,post}$ has the same value as $R_{125,post}$ different recovery strategies under this scenario are studied. The calculated indices are shown in Tables 9 and 10. From the results, we can find that the optimal recovery strategies are 121-183-184-125 and 125-183-184-121.

Similar to the RTS-79 case, the system resilience r_2 of each recovery strategy are calculated and tabulated in Tables 11 and 12. From the results, it can be concluded that the best recovery strategies are 121-183-184-125 and 125-183-184-121 in Case 1, and 121&183-125&184 and 125&183-121&184 in Case 2. Specifically, the system resilience of recovery strategies 121-183-184-125 and 125-183-184-121 are 97.24% in Case 1, while the value is 97.24% for the strategies 121&183-125& 184 and 125&183-121&184 in Case 2.

5. Conclusion

In this paper, a resilience assessment approach are proposed using an impact-increment-based state enumeration method. Two resilience indices are developed from the perspectives of the system and individual component levels, respectively. The system resilience indices are used to quantify the expected consequence of extreme disruptions from a system-wide perspective. For a system with insufficient resilience, the component resilience indices, including the pre-disruption and post-disruption indices, are proposed to determine the weak points of the entire system. Specifically, the pre-disruption indices are used to

determine the weak points of the system before the occurrence of disruptions, while the post-disruption indices are leveraged for designing the optimal recovery strategies. Comparative results carried out on the IEEE RTS-79 and the IEEE-118 systems validate the effectiveness of the proposed approach with the consideration of different transmission line failure scenarios. In our future work, the reduction of higher-order contingency states with independent outage components will be investigated to further improve the computational efficiency while maintaining high calculation accuracy. In addition, the advent of microgrids (MGs) in modern power systems has introduced promising measures that can fulfill the resiliency requirements. We will extend our research to address distribution system and microgrids resilience assessment in the future.

CRediT authorship contribution statement

Xiaonan Liu: Methodology, Software, Validation, Investigation, Writing - original draft. Kai Hou: Conceptualization, Writing - review & editing, Supervision. Hongjie Jia: Supervision, Project administration, Funding acquisition. Junbo Zhao: Writing - review & editing, Supervision. Lamine Mili: Conceptualization, Writing - review & editing. Yunfei Mu: Writing - review & editing. Jusong Rim: Writing - review & editing. Yunkai Lei: Funding acquisition.

Declaration of Competing Interest

None.

Acknowledgments

This work was supported by the National Natural Science Foundation of China (Grant No. 51707129), the National Science Fund for Distinguished Young Scholars (Grant No. 51625702), Natural Science Foundation of Tianjin City (Grant No. 18JCQNJC07600), and the Joint Funds of the National Natural Science Foundation of China (Grant No. U1766210).

APPENDIX

A 3-bus transmission system is used as an example. The expected impacts of all failure scenarios can be obtained by

$$R_{\text{SVS}} = u_1 \Delta I_1 + u_2 \Delta I_2 + u_3 \Delta I_3 + u_1 u_2 \Delta I_{12} + u_1 u_3 \Delta I_{13} + u_2 u_3 \Delta I_{23} + u_1 u_2 u_3 \Delta I_{123}$$

$$\tag{13}$$

 R_{sys} can be divided into two parts: one is related to Line-1 and the other is independent from it. Thus, (13) can be transformed into

$$R_{\text{sys}} = (u_1 \Delta I_1 + u_1 u_2 \Delta I_{12} + u_1 u_3 \Delta I_{23} + u_1 u_2 u_3 \Delta I_{123}) + (u_2 \Delta I_2 + u_3 \Delta I_3 + u_2 u_3 \Delta I_{23})$$

$$= u_1 (\Delta I_1 + u_2 \Delta I_{12} + u_3 \Delta I_{23} + u_2 u_3 \Delta I_{123}) + (u_2 \Delta I_2 + u_3 \Delta I_3 + u_2 u_3 \Delta I_{23})$$
(14)

If Line-1 will not fail during the disruption, the expected impacts of other transmission line failures can be obtained by

$$R_{SVS}|_{u_1=0} = u_2 \Delta I_2 + u_3 \Delta I_3 + u_2 u_3 \Delta I_{23}$$
(15)

Subtract (15) from (14), all the impacts that are unrelated to Line-1 have been eliminated. Thus, the pre-disruption component resilience index of Line-1 $R_{1,pre}$ is expressed as

$$R_{1,pre} = u_1(\Delta I_1 + u_2\Delta I_{12} + u_3\Delta I_{13} + u_2u_3\Delta I_{123})$$
(16)

Similarly, $R_{2,pre}$ and $R_{3,pre}$ can be obtained respectively via

$$R_{2,pre} = u_2(\Delta I_2 + u_1 \Delta I_{12} + u_3 \Delta I_{23} + u_1 u_3 \Delta I_{123})$$
(17)

$$R_{3,pre} = u_3(\Delta I_3 + u_1 \Delta I_{13} + u_2 \Delta I_{23} + u_1 u_2 \Delta I_{123})$$
(18)

Then, assuming that all three lines have failed, the post-disruption component resilience index of Line-1 $R_{1,post}$ can be obtained by

$$R_{1,post} = R_{sys}|_{u_1 = 1, u_2 = 1, u_3 = 1} - R_{sys}|_{u_1 = 0; u_2 = 1, u_3 = 1}$$

$$= (\Delta I_1 + \Delta I_2 + \Delta I_3 + \Delta I_{12} + \Delta I_{13} + \Delta I_{23} + \Delta I_{123}) - (\Delta I_2 + \Delta I_3 + \Delta I_{23})$$

$$= \Delta I_1 + \Delta I_{12} + \Delta I_{13} + \Delta I_{123}$$

$$(19)$$

Likewise, $R_{2,post}$ and $R_{3,post}$ are given by

$$R_{2,post} = \Delta I_2 + \Delta I_{12} + \Delta I_{23} + \Delta I_{123} \tag{20}$$

$$R_{3,post} = \Delta I_3 + \Delta I_{13} + \Delta I_{23} + \Delta I_{123} \tag{21}$$

Assuming that the repair time of each transmission line equals to t_1 , t_2 , t_3 , respectively. Then the enhanced resiliencies are equal to $R_{1,post}^*t_1$, $R_{2,post}^*t_2$ and $R_{3,post}^*t_3$ when each transmission line has been repaired, respectively.

If the resilience enhancement of Line-1 is the best, it will be repaired first. The post-disruption component resilience indices of the remaining two failed lines can be obtained by

$$R'_{2,post} = R_{\text{sys}}|_{u_2=1,u_3=1;u_1=0} - R_{\text{sys}}|_{u_2=0;u_3=1;u_1=0} = \Delta I_2 + \Delta I_{23}$$
(22)

$$R'_{3,post} = R_{sys}|_{u_3=1, u_2=1; u_1=0} - R_{sys}|_{u_3=0; u_2=1; u_1=0} = \Delta I_3 + \Delta I_{23}$$
(23)

If $R'_{2,post} > R'_{3,post}$, Line-2 is repaired followed by Line-3.

Reference

- Panteli M, Mancarella P. Influence of extreme weather and climate change on the resilience of power systems: impacts and possible mitigation strategies. Elect Power Syst Res 2015;127:259–70.
- [2] Wang S, Ge L, Cai S, Wu L. Hybrid interval AHP-entropy method for electricity user evaluation in smart electricity utilization. J Modern Power Syst Clean Energy 2018;6(4):701–11.
- [3] Dobson I et al. IEEE PES CAMS task force on understanding, prediction, mitigation and restoration of cascading failures, Initial review of methods for cascading failure analysis in electric power transmission systems. IEEE PES GM, Pittsburg, PA, July; 2008.
- [4] Holling CS. Resilience and stability of ecological systems. Annu Rev Ecol Syst Nov. 1973;4:1–23.
- [5] Folke C. Resilience: the emergence of a perspective for social–ecological systems analyses. Global Environ Change 2006;16(3):253–67.
- [6] Francis R, Bekera B. A metric and frameworks for resilience analysis of engineered and infrastructure systems. Reliab. Eng. Syst. Safe. 2014;121:90–103.
- [7] Mili L, Triantis K, Greer A. Integrating community resilience in power system planning. Chapter 9 of the book edited by V. Badescu, G. C. Lazaroiu, L. Barelli, Power Engineering: Advances and Challenges: Part B Electrical Power, 1st ed. CRC Press: 2019.
- [8] Bruneau M, Chang SE, Eguchi RT, Lee GC, O'Rourke TD, Reinhorn AM, et al. A framework to quantitatively assess and enhance the seismic resilience of communities. Earthq Spectra 2003;19(4):733–52.
- [9] Bruneau M, Reinhorn AM. Exploring the concept of seismic resilience for acute care facilities. Earthq Spectra 2007;23(1):41–62.
- [10] Cimellaro G, Reinhorn A, Bruneau M. Framework for analytical quantification of disaster resilience. Eng Struct 2010;32(11):3639–49.
- [11] Panteli M, Mancarella P, Trakas D, Kyriakides E, Hatziargyriou N. Metrics and quantification of operational and infrastructure resilience in power systems. IEEE

- Trans Power Syst 2017;32(6):4732-41.
- [12] Panteli M, Pickering C, Wilkinson S, Dawson R, Mancarella P. Power system resilience to extreme weather: fragility modelling, probabilistic impact assessment, and adaptation measures. IEEE Trans Power Syst 2017;32(5):3747–57.
- [13] Panteli M, Mancarella P, Wilkinson S, Dawson R, Pickering C. Assessment of the resilience of transmission networks to extreme wind events, IEEE Power Tech 2015. Netherlands: Eindhoven; 2015.
- [14] Panteli M, Mancarella P. Operational resilience assessment of power systems under extreme weather and loading conditions. IEEE PES General Meeting 2015, Denver, USA, 26-30; Jul. 2015.
- [15] Panteli M, Mancarella P. Modelling and evaluating the resilience of critical electrical power infrastructure to extreme weather events. IEEE Syst J 2017;11(3):1733–42.
- [16] Ouyang M, Duenas-Osorio L. Time-dependent resilience assessment and improvement of urban infrastructure systems. Chaos 2012;22(3):33–122.
- [17] Ouyang M, Duenas-Osorio L, Min X. A three-stage resilience analysis framework for urban infrastructure systems. Struct Saf 2012;36–37(2): 23–31.
- [18] Ouyang M, Duenas-Osorio L. Multi-dimensional hurricane resilience assessment of electric power systems. Struct Saf 2014.;48:15–24.
- [19] Amirioun MH, Aminifar F, Shahidehpour M. Resilience-promoting proactive scheduling against hurricanes in multiple energy carrier microgrids. IEEE Trans Power Syst 2019;34(3):2160–8.
- [20] Amirioun MH, Aminifar F, Lesani H. Towards proactive scheduling of microgrids against extreme floods. IEEE Trans Smart Grids 2018;9(4): 3900–2.
- 21] Amirioun MH, Aminifar F, Lesani H, Shahidehpour M. Metrics and quantitative framework for assessing microgrid resilience against windstorms. Int J Electr Power Energy Syst 2019;104:716–23.
- 22] Amirioun MH, Aminifar F, Lesani H. Resilience-oriented proactive management of microgrids against windstorms. IEEE Trans Power Syst 2018;33(4):4275–84.
- [23] Liu X, Hou K, Jia H, Mu Y, Yu X, Wang Y, et al. A quantified resilience assessment approach for electrical power systems considering multiple transmission line outages. In: IEEE Elect power energy conf 1-5; Oct. 2017.

- [24] Gholami A, et al. Toward a consensus on the definition and taxonomy of power system resilience. IEEE Access 2018;6(1):32035–53.
- [25] Hou K, Jia H, Li X, Xu X, Mu Y, Tao J, et al. Impact-increment based decoupled reliability assessment approach for composite generation and transmission systems. IET Gener Transm Distrib Feb. 2018;12(3):586–95.
- [26] Hou K, Jia H, Yu X, Zhu L, Xu X, Li X. An impact increment-based state enumeration reliability assessment approach and its application in transmission systems. IEEE PES GM; 2016. July 17-21, Boston, MA, USA.
- [27] Hou K, Jia H, Yu X, Li Y, Xie C, Yan J. "Composite generation and transmission system reliability assessment using impact increment-based state enumeration method. In: Int conf on probabilistic methods applied to power syst (PMAPS), Beijing, China; 2016. October 16–20.
- [28] Lei Y, Zhang P, Hou K, Jia H, Mu Y, Sui B. An incremental reliability assessment approach for transmission expansion planning. IEEE Trans Power Syst 2018.;33(3):2597–609.
- [29] Bie Z, Lin Y, Li G, Li F. Battling the extreme: a study on the power system resilience. Proc IEEE 2017;105(7):1253–66.
- [30] Song X, Wang Z, Gan D, Qiu J. Transient stability risk assessment of power grid

- under typhoon weather. Power Syst Protect Control 2012;40(24):1-8.
- [31] Billinton R, Allan RN. Reliability evaluation of engineering systems: concepts and techniques; 1983. p. 253–81.
- [32] Panteli M, Trakas DN, Mancarella P, Hatziargyriou ND. Power systems resilience assessment: hardening and smart operational enhancement strategies. Proc IEEE, vol. 105, no. 7; July 2017.
- [33] Panteli M, Mancarella P. The grid: stronger, bigger, smarter? Presenting a conceptual framework of power system resilience. IEEE Power Energy Mag, vol. 13, no. 3; May-Jun. 2015. p. 58–66.
- [34] Grigg C, Wong P, Albrecht P, Allan R, Bhavaraju M, Billinton R, et al. The IEEE reliability test system 1996. A report prepared by the reliability test system task force of the application of probability methods subcommittee. IEEE Trans Power Syst 1999;14(3):1010–20.
- [35] Lieber D, Nemirovskii A, Rubinstein RY. A fast Monte Carlo method for evaluating reliability indexes. IEEE Trans Reliab 1999;48(3):256–61.
- [36] IEEE 118-Bus System, IIIinois center for a smarter electric grid. [Online]. Available: < http://publish.illinois.edu/smartergrid/ieee-118-bus-system/ > .